PHYSICAL REVIEW D **83,** 095020 (2011)

# Associated central exclusive production of charged Higgs bosons

Rikard Enberg* and Roman Pasechnik†

*Department of Physics and Astronomy, Uppsala University, Box 516, SE-751 20 Uppsala, Sweden*
(Received 11 April 2011; published 25 May 2011)

We propose central exclusive production of a charged Higgs boson in association with a $W$ boson as a possible signature of certain types of extended Higgs sectors. We calculate the cross section and find that the rate at the LHC could be large enough to allow observation in some models with two-Higgs doublets, where the charged Higgs and at least one of the neutral scalars can be light enough. We use the two-Higgs doublet model as a prototype and consider two distinct regions of parameter space, but we also briefly discuss the prospects for the next-to-minimal supersymmetric standard model, where the charged Higgs may very well be quite light.

DOI: 10.1103/PhysRevD.83.095020 PACS numbers: 14.80.Fd, 12.38.−t

## I. INTRODUCTION

The Higgs sector of the standard model (SM) contains a single scalar doublet, which leads to one physical, neutral Higgs boson after electroweak symmetry breaking. Additional Higgs bosons, and, in particular, a charged Higgs boson, are predicted in many models for physics beyond the standard model with extended Higgs sectors, such as the minimal and the next-to-minimal supersymmetric standard models (MSSM and NMSSM, respectively). The detection of a charged scalar would be clear evidence of physics beyond the standard model. The MSSM contains one additional Higgs doublet, but supersymmetry places quite severe restrictions on the parameters of the model and their relations, and enforce a Higgs sector of a special kind, to be discussed below (the sizable loop corrections change this picture, however). In the NMSSM, the Higgs sector contains an additional singlet which allows for a larger variety of parameters.

It is phenomenologically interesting to consider a more minimal addition to the SM, namely, adding only one additional Higgs doublet to the SM. In this two-Higgs doublet model (2HDM), three of the 8 degrees of freedom give masses to the vector bosons, and five physical Higgs bosons remain: in a $CP$-conserving theory these are the $CP$-even neutral scalars $h^0$ and $H^0$, the $CP$-odd $A^0$, and the charged Higgs bosons $H^{\pm}$ (see [1,2] for reviews). This is a minimal extension of the Higgs sector but it leads to a rich phenomenology and is very useful as a laboratory for Higgs physics.

The central exclusive production (CEP) process $pp \to p + X + p$, where $X$ stands for a centrally produced system separated from the two very forward protons by large rapidity gaps, has been proposed [3] as an alternative way of searching for the neutral Higgs boson (see [4] for a review). The Higgs boson is produced in the $gg \to H$ subprocess through a quark loop. The two incoming protons survive the collision and lose only a small fraction of their original momentum. This means that the overall $t$-channel exchange must be a color singlet, and this process is therefore very closely related to diffractive processes. If the momenta of the outgoing protons are measured by forward proton detectors placed far away from the interaction point, the mass of the $X$ system may be reconstructed [5] with a resolution of about 2 GeV per event [6]. This is the proposal of the FP420 project [6] which aims at placing detectors at 220 m and at 420 m away from ATLAS or CMS. The perturbative QCD description of the CEP process began in [7], and the calculation that is now commonly used was initiated by Khoze, Martin, and Ryskin and collaborators in [8]. It leads to a cross section for the standard model Higgs of about 3 fb at $\sqrt{s} = 14$ TeV for $m_H \sim 120$ GeV, but extensions of the standard model such as the MSSM can yield larger cross sections. This Durham model has later been applied for production of $\chi_c$ [9], gluon [10] and heavy quark dijets [11], etc., and has been compared with data from the Tevatron [12]. We will use this standard theoretical description in what follows.

One of the main motivations for considering central exclusive Higgs production is that in inclusive Higgs searches, using the decay $H \to b\bar{b}$ is complicated due to the huge background from QCD jets. In CEP, there is a suppression of $b\bar{b}$ production from QCD events due to spin-parity conservation in the forward limit. However, recent studies of various sources of irreducible $b\bar{b}$ background [11] have revealed a potential problem at low statistics, as the signal-to-background ratio turns out to be close to 1 whereas the absolute cross section is of the order of 1 fb. However, the overall theoretical uncertainty is rather large (an uncertainty of about a factor of 25 is claimed in Ref. [13]) and it is possible that the cross section is larger. This situation makes it interesting to consider other possible ways to probe the Higgs sector in CEP.

In this paper, we therefore propose a new potentially interesting channel, namely, central exclusive production of the charged Higgs boson in association with a $W$ boson.

*rikard.enberg@physics.uu.se
†roman.pasechnik@fysast.uu.se

 

This is a standard process in inclusive searches, and we will show below that the CEP cross section is large enough in some regions of parameter space to be useful at the LHC. If the charged Higgs would be observed this way, it would give important information on the properties of the Higgs sector.

To be specific, we choose to use the 2HDM as a prototype in our calculations. We will make one simplification. As we are here interested in examining the feasibility of the associated production channel, we want to consider the maximum possible cross sections. These occur when there is an $s$-channel resonance involved, and cross sections away from the resonance are bound to be smaller. We will therefore concentrate on the case when the cross section is resonantly enhanced. It has been shown [14] that in some regions of the parameter space of 2HDMs, the associated production cross section can be enhanced compared with the MSSM by orders of magnitude.

Our results can be seen as a proof of principle, but can be applied to more general models for physics beyond the SM. In particular, we will briefly discuss the NMSSM as one interesting example.

## II. THE TWO-HIGGS DOUBLET MODEL

The general two-Higgs doublet model (2HDM) has two scalar doublets $\Phi_{1,2}$ with the same hypercharge $Y = 1$. Setting parameters that break the $\mathbb{Z}_2$ symmetry explicitly to zero but keeping the soft-breaking parameter $m_{12}^2$, the most general scalar potential is given by

$$\begin{aligned}\mathcal{V} = {} & m_{11}^2\Phi_1^\dagger\Phi_1 + m_{22}^2\Phi_2^\dagger\Phi_2 - [m_{12}^2\Phi_1^\dagger\Phi_2 + \text{H.c.}] \\ & + \frac{1}{2}\lambda_1(\Phi_1^\dagger\Phi_1)^2 + \frac{1}{2}\lambda_2(\Phi_2^\dagger\Phi_2)^2 \\ & + \lambda_3(\Phi_1^\dagger\Phi_1)(\Phi_2^\dagger\Phi_2) + \lambda_4(\Phi_1^\dagger\Phi_2)(\Phi_2^\dagger\Phi_1) \\ & + \frac{1}{2}\Big[\lambda_5(\Phi_1^\dagger\Phi_2)^2 + \text{H.c.}\Big], \end{aligned} \tag{1}$$

where all parameters are real for $CP$-conserving models. Minimizing the potential and parametrizing the doublets in terms of the physical states, one finds relations for the masses of the Higgs bosons in terms of $\tan\beta = v_2/v_1$, the ratio of the vacuum expectation values of the two doublets, and the parameters of the potential. The two $CP$-even scalars $h^0$ and $H^0$ mix, with mixing angle $\alpha$. However, $\alpha$ only appears in the couplings between Higgs bosons and gauge bosons in the combinations $\sin(\beta - \alpha)$ and $\cos(\beta - \alpha)$. One should keep in mind that $\tan\beta$ is not *a priori* a physical parameter, and the potential (1) is in fact invariant under U(2) rotations of the doublets. In specific models, however, a specific basis, and thus a specific value of $\tan\beta$, is singled out as a physical parameter.

For completely general Yukawa couplings of the different Higgs bosons, one encounters unacceptably large flavor-changing neutral currents mediated by Higgs exchange. Glashow and Weinberg showed [15] that these vanish if each fermion only couples to one Higgs doublet, and one therefore usually defines four types of 2HDM, fancifully called type I, II, III and IV, or sometimes Y and X for the last two. The MSSM is at tree level a type II model, where the up- and down-type fermions couple to different doublets; however, this situation is changed somewhat by large loop corrections. In type I, instead, all fermions couple to the same doublet. In the following we will consider both type I and type II models.

In order for the central exclusive production mechanism to have a cross section in the interesting range, the mass of the charged Higgs boson must be relatively low. The experimental bounds on $m_{H^+}$ are the strictest in the type II model, where one has, roughly, $m_{H^+} \gtrsim 300$ GeV [16,17]. In the type I model, however, for $\tan\beta \gtrsim 2$–3 there is essentially no bound beyond the model independent bound that $m_{H^+} \gtrsim 80$ GeV [17]. For this reason, we shall take the type I model as our principal prototype. It could also be interesting to consider the type $X$ model, where $H^+$ can also be light, see e.g. [18] for a detailed study of its phenomenology. The type I results we show below correspond to models that are allowed by all existing data.

Because it is hard to find regions in the MSSM parameter space where the charged Higgs is light, we shall not consider the MSSM here. In the next-to-minimal supersymmetric standard model (NMSSM) on the other hand, the charged Higgs can easily be quite light (see e.g. [19–21]), and central exclusive production can be interesting. Supersymmetric models also have a contribution to the production amplitudes from squark loops, which can potentially be large and positive.

To keep the analysis simple, we will leave a detailed study of NMSSM, and supersymmetric models in general, for the future. Instead we will, in addition to the type I results, also show results for the 2HDM type II model, which is more similar to SUSY models. However, note that these type II results are not to be taken literally, since they have light charged Higgs bosons that are not allowed by flavor data. The reason that we still find this interesting is that in the NMSSM the charged Higgs is allowed to be light. The type II results should therefore be seen as an example.

### A. Couplings

In the type I model, the fermions get their masses from only one of the Higgs doublets. The dependence of the Yukawa couplings on $\alpha$ and $\beta$ is therefore the same for the up and down-type fermions. If the mixing $\alpha$ is either zero or $\pi/2$, the $H^0$ or the $h^0$ does not couple to the fermions at all. The Yukawa couplings of the three neutral scalars to top and bottom quarks relative to the couplings of the SM Higgs boson $\phi^0$ are in the type I model given by

$$\lambda_{\text{I},t}^{h^0} = \lambda_{\text{I},b}^{h^0} = \frac{\cos\alpha}{\sin\beta} \tag{2}$$

$$\lambda_{\mathrm{I},t}^{H^0} = \lambda_{\mathrm{I},b}^{H^0} = \frac{\sin\alpha}{\sin\beta} \tag{3}$$

$$\lambda_{\mathrm{I},t}^{A^0} = i\gamma_5 \cot\beta \tag{4}$$

$$\lambda_{\mathrm{I},b}^{A^0} = -i\gamma_5 \cot\beta. \tag{5}$$

In the type II model there is the well-known large $\tan\beta$-enhancement of the down-type fermion couplings. The corresponding couplings are then

$$\lambda_{\mathrm{II},t}^{h^0} = \frac{\cos\alpha}{\sin\beta} \tag{6}$$

$$\lambda_{\mathrm{II},b}^{h^0} = -\frac{\sin\alpha}{\cos\beta} \tag{7}$$

$$\lambda_{\mathrm{II},t}^{H^0} = \frac{\sin\alpha}{\sin\beta} \tag{8}$$

$$\lambda_{\mathrm{II},b}^{H^0} = \frac{\cos\alpha}{\cos\beta} \tag{9}$$

$$\lambda_{\mathrm{II},t}^{A^0} = i\gamma_5 \cot\beta \tag{10}$$

$$\lambda_{\mathrm{II},b}^{A^0} = i\gamma_5 \tan\beta. \tag{11}$$

The couplings in the type I model are thus the same as the couplings to the up-type quarks in the type II model. As it is $\sin(\beta-\alpha)$ that enters the gauge boson couplings, it is useful to write these relations in terms of $\sin(\beta-\alpha)$, $\cos(\beta-\alpha)$ and $\tan\beta$ only,

$$\frac{\sin\alpha}{\sin\beta} = \cos(\beta-\alpha) - \cot\beta\sin(\beta-\alpha) \tag{12}$$

$$\frac{\cos\alpha}{\sin\beta} = \sin(\beta-\alpha) + \cot\beta\cos(\beta-\alpha) \tag{13}$$

$$\frac{\cos\alpha}{\cos\beta} = \cos(\beta-\alpha) + \tan\beta\sin(\beta-\alpha) \tag{14}$$

$$\frac{\sin\alpha}{\cos\beta} = -\sin(\beta-\alpha) + \tan\beta\cos(\beta-\alpha). \tag{15}$$

The other important parameter for our scattering process is the coupling of the neutral scalars to the charged Higgs and $W$. These are the same for all types of 2HDM, and as for all Higgs-Higgs-vector couplings, they are proportional to $\cos(\beta-\alpha)$ for $h^0$ and to $\sin(\beta-\alpha)$ for $H^0$.

## III. THE HARD SUBPROCESS

There are four diagrams that contribute to the hard subprocess amplitude $gg\to H^\pm W^\mp$ at the one-loop level, when requiring the two incoming gluons to be in a color singlet state. These are depicted in Fig. 1 and 2. The amplitudes for this process have been computed for inclusive associated production by Barrientos Bendezú and Kniehl [22] (see also [23,24] for the MSSM results). In the rest of this section we give results for the type I model modified from Ref. [22]. The corresponding formulas for the type II model can be found in that paper.

The amplitude for $gg\to H^\pm W^\mp$ given by the sum of the triangle diagrams in Fig. 1 is

$$V_{\lambda_W} = \frac{\sqrt{2}}{\pi}\alpha_s(\mu)G_F m_W \epsilon_\gamma^*(p_W)(q_1+q_2)^\gamma \epsilon_\mu^c(q_1)\epsilon_\nu^c(q_2) \times\Big[\Big(q_2^\mu q_1^\nu - \frac{\hat{s}}{2}g^{\mu\nu}\Big)\Sigma(\hat{s}) + i\epsilon^{\mu\nu\rho\sigma}q_{1\rho}q_{2\sigma}\Pi(\hat{s})\Big], \tag{16}$$

where $\alpha_s(\mu)$ is the strong coupling, $\hat{s}=M_{HW}^2$ is the invariant mass squared of the $H^\pm W^\mp$ pair, $\mu$ is the renormalization scale, $\epsilon_\gamma^*$ is the polarization vector of the $W$ boson with momentum $p_W$ and helicity $\lambda_W$, and $\epsilon_{\mu,\nu}^c$ are the polarization vectors of the gluons with momenta $q_{1,2}$. These are summed over the color index $c$. The functions $\Sigma$ and $\Pi$ come from the loop integration and correspond to $h^0$ and $H^0$ exchange ($\Sigma$) and $A^0$ exchange ($\Pi$) in the $s$ channel. They are given by

$$\Sigma(\hat{s}) = \sum_{q=t,b}\mathcal{S}(\hat{s})S\Big(\frac{\hat{s}+i\epsilon}{4m_q^2}\Big) \tag{17}$$

$$\Pi(\hat{s}) = \sum_{q=t,b}\mathcal{P}_q(\hat{s})P\Big(\frac{\hat{s}+i\epsilon}{4m_q^2}\Big), \tag{18}$$

where the functions

$$S(r) = \frac{1}{r}\Big[1-\Big(1-\frac{1}{r}\Big)\mathrm{arcsinh}^2\sqrt{-r}\Big] \tag{19}$$

$$P(r) = -\frac{1}{r}\mathrm{arcsinh}^2\sqrt{-r} \tag{20}$$

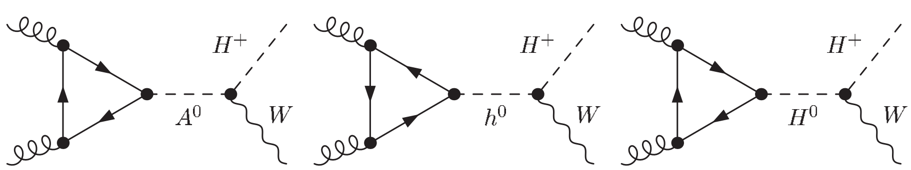


FIG. 1. Subprocesses involving an $s$-channel Higgs boson.

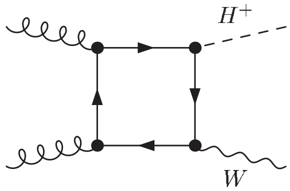


FIG. 2. The box diagram.

must be continued analytically for three regions in $r$, such that for $r \leq 0$, $0 < r \leq 1$, or $r > 1$ one must use $\text{arcsinh}\sqrt{-r}$, $-i\arcsin\sqrt{r}$, or $\text{arccosh}\sqrt{r} - i\pi/2$. The functions $\mathcal{S}$ and $\mathcal{P}$ contain the propagators and relative couplings and are defined as

$$\mathcal{S}(\hat{s}) = \frac{1}{\sin\beta}\left(\frac{\cos\alpha\cos(\alpha-\beta)}{\hat{s} - m_{h^0}^2 + i m_{h^0}\Gamma_{h^0}} + \frac{\sin\alpha\sin(\alpha-\beta)}{\hat{s} - m_{H^0}^2 + i m_{H^0}\Gamma_{H^0}}\right) \tag{21}$$

$$\mathcal{P}_t(\hat{s}) = \frac{\cot\beta}{\hat{s} - m_{A^0}^2 + i m_{A^0}\Gamma_{A^0}}, \tag{22}$$

and $\mathcal{P}_b(\hat{s}) = -\mathcal{P}_t(\hat{s})$. We have modified the $\mathcal{S}$, $\mathcal{P}$ functions given in [22] with the appropriate Yukawa couplings for type I. Thus the $t$ and $b$ functions are identical in our case. However, the contribution from $b$ is negligible, since the $S$ and $P$ functions tend to zero for $r \to \infty$, and there is no $\tan\beta$ enhancement in type I.

We do not list the complicated expressions for the box diagrams, schematically shown in Fig. 2.

As discussed above, if the mass relations are such that one of the intermediate Higgs bosons $h^0$, $H^0$ or $A^0$ is close in mass to the $H^\pm W^\mp$ system, the three resonant triangle diagrams in Fig. 1 will completely dominate the amplitude. We have checked this fact by calculating the hard $gg \to H^\pm W^\mp$ subprocess cross section at the $h^0$ and $H^0$ resonances in two ways: exactly, with triangle and box diagrams included, and keeping triangles only. These calculations were performed using FeynArts and FormCalc [25]. The relative numerical difference between these two cross sections is extremely small, on the order of $10^{-6}$, meaning that the interference between triangles and boxes at the Higgs resonance is totally negligible. In this paper we will concentrate on scenarios that yield the largest possible cross sections, and we will therefore neglect the box diagrams.

In inclusive associated production, all three triangle diagrams contribute to the amplitude. This is not the case for central exclusive production, which occurs in the forward limit. As we will show below, the amplitude with an $s$-channel $A^0$ boson vanishes in this limit due to its $CP$-odd nature. We therefore only need to consider the amplitudes with exchange of $h^0$ and $H^0$.

## IV. CENTRAL EXCLUSIVE PRODUCTION

We follow the QCD mechanism for central exclusive production, initially developed by Khoze, Martin and Ryskin (KMR) in Refs. [8]. A schematic diagram for central exclusive associated $H^\pm W^\mp$ pair production in proton-proton scattering $pp \to pH^\pm W^\mp p$ is shown in Fig. 3.

The momenta of the intermediate gluons are given by Sudakov decompositions in terms of the incoming proton momenta $p_{1,2}$:

$$q_1 = x_1 p_1 + q_{1\perp}, \qquad q_2 = x_2 p_2 + q_{2\perp},$$
$$q_0 = x' p_1 - x' p_2 + q_{0\perp} \simeq q_{0\perp}, \qquad x' \ll x_{1,2}, \tag{23}$$

such that $q_\perp^2 \simeq -|\mathbf{q}|^2$. Here, and below, we write transverse 2-momenta in boldface. In the forward scattering limit, we have

$$t_{1,2} = (p_{1,2} - p'_{1,2})^2 = p'^2_{1/2\perp} \to 0,$$
$$q_{0\perp} \simeq -q_{1\perp} \simeq q_{2\perp}. \tag{24}$$

According to the KMR approach, we write the amplitude of this process, which in the diffractive limit is dominated by its imaginary part, as

$$\mathcal{M}_{\lambda_W} \simeq is\frac{\pi^2}{2}\frac{1}{N_c^2 - 1}\int d^2\mathbf{q}_0 V_{\lambda_W}\frac{f_g(q_0, q_1) f_g(q_0, q_2)}{\mathbf{q}_0^2\mathbf{q}_1^2\mathbf{q}_2^2},$$

where $\lambda_W$ is the helicity of produced $W^\pm$ boson, $f_g(r_1, r_2)$ is the off diagonal unintegrated gluon distribution function (UGDF), which is dependent on the longitudinal and transverse components of both gluons $r_1$ and $r_2$ emitted from the proton line. The $gg \to H^\pm W^\mp$ hard subprocess amplitude $V_{\lambda_W}$ in given by Eq. (16). The diffractive amplitude (25) is averaged over the color indices and over the two transverse polarizations of the incoming gluons.

The bare amplitude above is subject to absorption corrections which depend on the collision energy and the typical proton transverse momenta. In the original KMR calculations the bare production cross section is simply multiplied by a gap survival factor, which is estimated to be $\hat{S}^2 \simeq 0.015$ at the LHC energy [26].

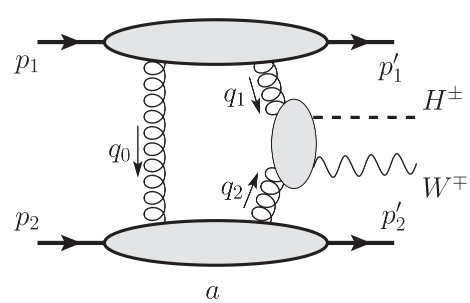


FIG. 3. The central exclusive $H^\pm W^\mp$ pair production. Typical contributions to the hard subprocess scattering amplitude $gg \to H^\pm W^\mp$ are shown in Figs. 1 and 2.

### A. Unintegrated gluon distributions

The coupling of the gluons to the proton is described in terms of the off diagonal unintegrated gluon distribution functions (UGDFs) $f_g(q_0, q_{1,2}) = f_g^{\rm off}(x', x_{1,2}, \mathbf{q}_{1,2}^2, \mathbf{q}_0^2, \mu_F^2; t_{1,2})$ at the factorization scale $\mu_F \sim M_{HW} \gg |\mathbf{q}_0|$. In the forward (24) and asymmetric limit of small $x' \ll x_{1,2}$, where $x'$ is the longitudinal momentum fraction of the screening gluon, the off diagonal UGDF is written as a skewedness factor $R_g$ multiplying the diagonal UGDF, which describes the coupling of gluons with momentum fractions $x_{1,2}$ to the proton (see Refs. [27,28] for details). The skewedness parameter $R_g \simeq 1.2$–$1.3$ is expected to be roughly constant at LHC energies and gives only a small contribution to the overall normalization uncertainty.

In the kinematics considered here, the unintegrated gluon density can be written in terms of the conventional gluon distribution $g(x, \mathbf{q}^2)$ as [28]

$$f_g(x, \mathbf{q}^2, \mu_F^2) = \frac{\partial}{\partial \ln\mathbf{q}^2}\left[xg(x, \mathbf{q}^2)\sqrt{T_g(\mathbf{q}^2, \mu_F^2)}\right], \quad (25)$$

where $T_g$ is the Sudakov form factor which suppresses real emissions during the evolution, so that the rapidity gaps are not populated by gluons. It is given by

$$T_g(\mathbf{q}^2, \mu_F^2) = \exp\biggl(-\int_{\mathbf{q}^2}^{\mu_F^2}\frac{d\mathbf{k}^2}{\mathbf{k}^2}\frac{\alpha_s(\mathbf{k}^2)}{2\pi} \times \int_0^{1-\Delta}\biggl[zP_{gg}(z) + \sum_q P_{qg}(z)\biggr]dz\biggr), \quad (26)$$

where $\Delta$ in the upper limit is taken to be [29]

$$\Delta = \frac{|\mathbf{k}|}{|\mathbf{k}| + M_{HW}}. \quad (27)$$

### B. CEP as a spin-parity analyzer

Because of its $CP$-odd nature, the central exclusive $A^0$ production is suppressed in the forward limit due to what has become known as the $J_z = 0$ selection rule [8]. To demonstrate this, let us calculate explicitly the hard subprocess part $V_{\lambda_W}$ (16) describing the scattering of two basically on shell gluons into an $H^\pm W^\mp$ pair. Summing over colors and polarizations of the gluons, we have

$$V_{\lambda_W} = (N_c^2 - 1)\frac{\sqrt{2}}{\pi}\alpha_s(\mu)G_F m_W \epsilon_\gamma^*(p_W)(q_1 + q_2)^\gamma n_\mu^- n_\nu^+ \times\biggl[\biggl(q_2^\mu q_1^\nu - \frac{\hat{s}}{2}g^{\mu\nu}\biggr)\Sigma(\hat{s}) + i\epsilon^{\mu\nu\rho\sigma}q_{1\rho}q_{2\sigma}\Pi(\hat{s})\biggr],$$
$$n_\mu^\mp = \frac{p_{1,2}^\mu}{E_{p,\rm cms}}, \quad (28)$$

where by a convention we adopt the light cone vectors $n_\mu^\pm$ as transverse gluon polarization vectors, and where $E_{p,\rm cms} = \sqrt{s}/2$. Momentum conservation and gauge invariance imply that

$$\hat{s} = x_1x_2s \simeq 2(q_1q_2),$$
$$V_{\lambda_W} = n_\mu^- n_\nu^+ V^{\mu\nu} = \frac{4}{\hat{s}}q_{1\perp}^\mu q_{2\perp}^\nu V_{\mu\nu}.$$

A straightforward calculation leads to

$$V_{\lambda_W} = -(N_c^2 - 1)\frac{2\sqrt{2}}{\pi}\alpha_s(\mu)G_F m_W(\epsilon^*(p_W)\cdot p_H) \times\Bigl[(q_{1\perp}q_{2\perp})\Sigma(\hat{s}) + i(q_2^x q_1^y - q_2^y q_1^x)\Pi(\hat{s})\Bigr], \quad (29)$$

from which it is obvious that in the forward limit given by Eq. (24), the coefficient in front of $\Pi(\hat{s})$ disappears, so the contribution of $A^0$ to central exclusive $H^\pm W^\mp$ pair production vanishes, and only the $h^0$, $H^0$ contributions to $\Sigma(\hat{s})$ survive.

### C. $H^\pm W^\mp$ CEP cross section in the narrow-width approximation

As we consider resonance production, we use the narrow-width approximation in our calculation of the cross section, and therefore need the production cross section of $h^0$ and $H^0$. In the type I 2HDM, there is no large-$\tan\beta$ enhancement of Yukawa couplings to $b$-quarks; thus the contribution from $b$-quark loops to the $gg \to h^0, H^0$ process is negligible. The only difference between the CEP cross section for the standard model Higgs boson $H$ and for the 2HDM Higgs bosons $h^0$, $H^0$ is then through the Yukawa couplings defined in Eqs. (2) and (3). The central exclusive associated $H^\pm W^\mp$ production in the narrow-width approximation is then given by the contribution from the relevant resonance, either $h^0$ or $H^0$, as

$$\sigma_{HW}^{\rm CEP} \simeq \begin{cases} \sigma_{h_{\rm SM}}^{\rm CEP}(m_{h^0})(\lambda_{{\rm I},t}^{h^0})^2 & \times{\rm BR}(h^0 \to H^\pm W^\mp) \\ \sigma_{h_{\rm SM}}^{\rm CEP}(m_{H^0})(\lambda_{{\rm I},t}^{H^0})^2 & \times{\rm BR}(H^0 \to H^\pm W^\mp) \end{cases} \quad (30)$$

where $\sigma_{h_{\rm SM}}^{\rm CEP}(m_h)$ is the standard model Higgs boson CEP cross section calculated at a given Higgs mass $m_h$.

In the type II model, on the other hand, the contribution from $b$ quarks can be significant. Since we are working in the narrow-width approximation, the contribution from $b$-quark loops cannot be added coherently on the amplitude level. We therefore add this contribution on the cross section level, ignoring the interference terms. We estimate from the sizes of the couplings that this will give an error of less than 20%. A second approximation is that the cross section for the standard model Higgs is computed for $t$-quark loops only, and we now want to use this result for $b$-quark loops. Referring to Eq. (16) and the slow variation of the function $S(r)$, we estimate that the error we make here is less than 5%. Within these approximations, the central exclusive cross section for type II is then given, for $h^0$ or $H^0$, by

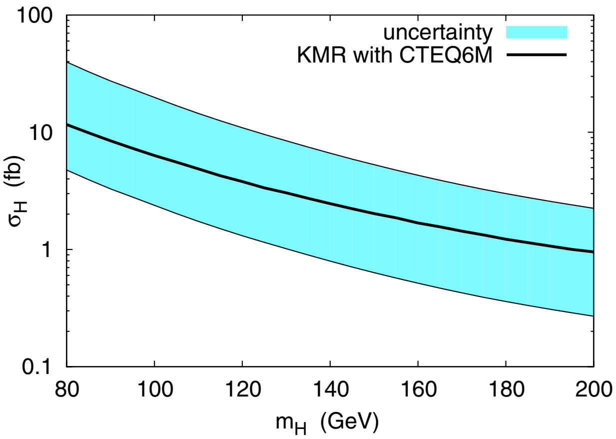


FIG. 4 (color online). Cross section for exclusive SM Higgs boson production at the LHC at 14 TeV as a function of the Higgs boson mass. The thick line is the KMR result obtained using the CTEQ6M pdf. The thin lines illustrate the theoretical uncertainty (about a factor of 10); see the description in the text.

$$\sigma_{HW}^{\rm CEP} \simeq \begin{cases} \sigma_{h_{\rm SM}}^{\rm CEP}(m_{h^0})[(\lambda_{{\rm II},t}^{h^0})^2 + (\lambda_{{\rm II},b}^{h^0})^2] \times {\rm BR}(h^0 \to H^\pm W^\mp) \\ \sigma_{h_{\rm SM}}^{\rm CEP}(m_{H^0})[(\lambda_{{\rm II},t}^{H^0})^2 + (\lambda_{{\rm II},b}^{H^0})^2] \times {\rm BR}(H^0 \to H^\pm W^\mp) \end{cases}. \quad (31)$$

We have checked that the narrow-width approximation works in the type I case by also computing the full $2 \to 4$ cross section $\sigma(pp \to pH^+W^-p)$ using the hard subprocess formulas in Eq. (16) and comparing with the results from Eq. (30) for some parameter points.

We will consider the cross section $\sigma_{h_{\rm SM}}^{\rm CEP}(m_h)$ calculated in the KMR model. The main sources of uncertainties are the unintegrated generalized gluon distribution, the gap survival probability factor, and the scale choice in the Sudakov form factor. In Fig. 4 we display the cross section for a SM Higgs boson as a function of the Higgs mass together with an uncertainty band. The upper line is given by the largest KMR result, as quoted in [4], which is obtained using the CTEQ6L parton distribution. The lower line is given by the smallest KMR result, as quoted in [13], which is obtained by using a modified scale choice in the Sudakov form factor, as prescribed in Ref. [29]. The uncertainty is roughly a factor ten.

The central line is the result we use in the present study. This line is given by the KMR result, quoted in [4], obtained by using the CTEQ6M parton distribution.

For a given point in the 2HDM parameter space we can thus easily obtain $\sigma_{HW}^{\rm CEP}$ using Eqs. (30) and (31).

## V. PARAMETER SCANS

In order to examine if the cross sections for the associated CEP can be large enough to be observed at LHC, we perform a simple scan over the parameter space of the model. For this purpose, we use the 2HDMC code [30] to compute the relevant parameters and masses of the considered models. 2HDMC is a public code that computes the masses and couplings of a general 2HDM from a specified set of input parameters of the potential, and also features a completely general Yukawa sector, which can also be restricted to type I, II, III or IV Yukawa sectors. It further includes both theoretical and experimental checks on the obtained model, and features a link to HiggsBounds [31] which allows further checks against collider data.

TABLE I. Parameter ranges in scan. Dimensionful parameters are given in GeV.

| | $m_{h^0}$ | $m_{A^0}$ | $m_{H^+}$ | $m_{12}^2$ | $\tan\beta$ | $\sin(\beta-\alpha)$ |
|---|---|---|---|---|---|---|
| lower | 115 | 10 | 88 | 500 | 3 | $-1$ |
| upper | 160 | 500 | 130 | 1500 | 5 | 1 |

We scan over the parameter space of type I and II two-Higgs doublet models in the physical basis, defined as the parameter basis where one replaces potential parameters $\lambda_i$ with the physical Higgs boson masses as input parameters. The parameters are then $m_{h^0}$, $m_{H^0}$, $m_{A^0}$, $m_{H^+}$, $m_{12}^2$, $\tan\beta$ and $\sin(\beta-\alpha)$. We choose points with $m_{H^0} = m_{H^+} + m_W$ to maximize the cross section in the $H^0$-exchange channel, and following the convention we are using, we impose $m_{h^0} < m_{H^0}$.

In the scan, we generate parameter points, choosing all parameters from a flat distribution within the limits shown in Table I. For each generated point we check positivity of the Higgs potential, unitarity at tree level and perturbativity. We further check the electroweak precision constraints on the oblique parameters $S$, $T$ and $U$ [32], the constraint on $g-2$ of the muon [33], and that the obtained Higgs masses are not ruled out by collider constraints. These checks are all performed using 2HDMC and HiggsBounds, and are applied to both the type I and type II models.

Additionally, one may take constraints from flavor physics into account. These constraints are not included in 2HDMC, but a detailed analysis has been published in Ref. [17]. The main flavor physics constraint for our purposes is that $\tan\beta > 3$, which is included in the choice of parameter limits. Note that, while all points we show for type I satisfy all constraints, as pointed out above, the type II model is ruled out by the flavor constraints and is shown instead as an example of a different type of Higgs sector, which can be relevant for extended versions of supersymmetry.

We generate $10^4$ points that pass the constraints. For each such point we compute the total central exclusive cross section using Eqs. (30) or (31). The results are shown in Fig. 5, where we show scatter plots of the cross section versus $\sin(\beta-\alpha)$, $\tan\beta$, $m_{H^+}$, and $m_{A^0}$ for both type I and type II.

Figure 5(a) shows that for $|\sin(\beta-\alpha)| \gtrsim 0.6$, the cross sections in the type II model are larger than 0.1 fb, and for

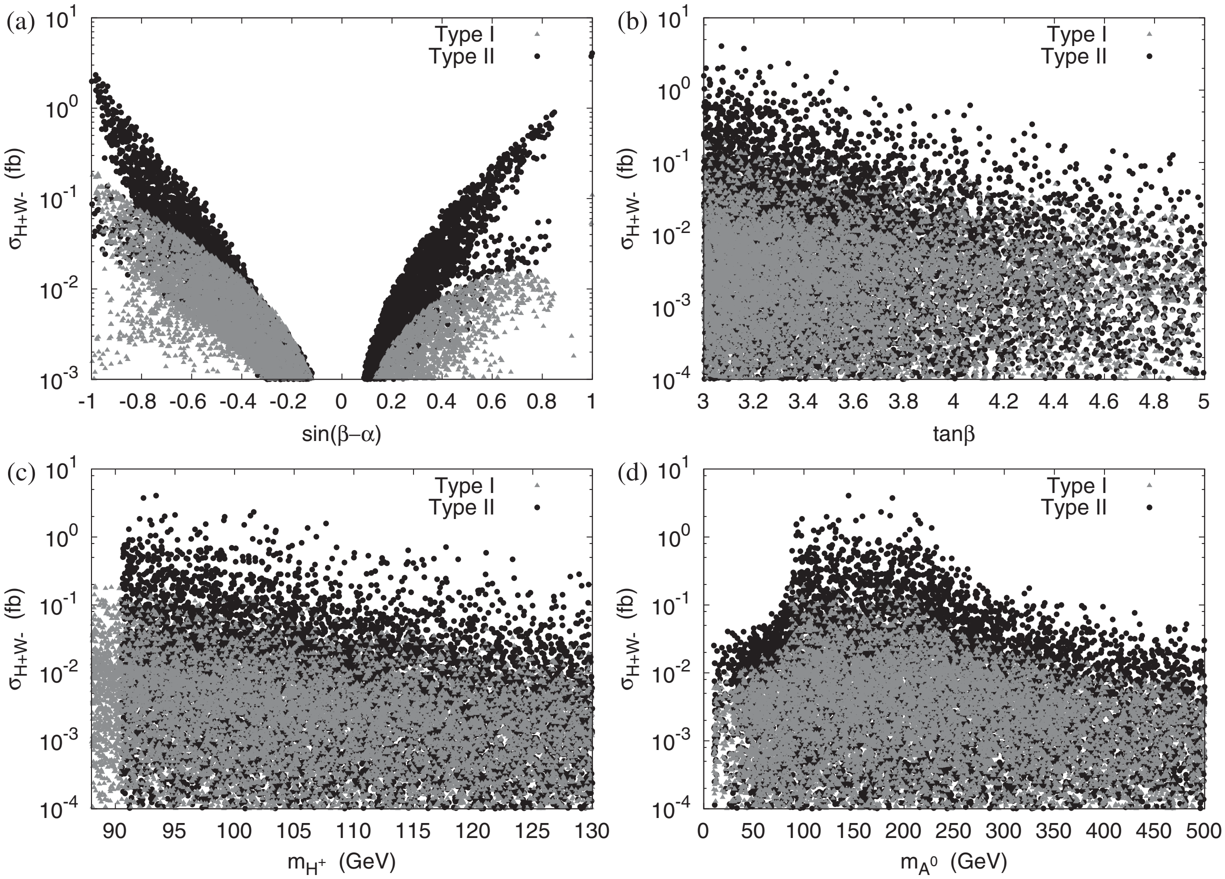


FIG. 5. Cross sections for central exclusive associated $H^+W^-$ production at $\sqrt{s} = 14$ TeV at the LHC for points in the parameter scan.

$\sin(\beta - \alpha) \lesssim -0.9$, they exceed 1 fb. The cross sections in the type I model do not vary as sharply with $\sin(\beta - \alpha)$, and are therefore smaller by factors of a few to a factor of 10.

The large cross sections occur in the region where the $h^0 - H^0$ mixing becomes small so that the coupling of the $H^0$ to the fermions is maximal and that of $h^0$ is minimal. In these regions, the cross sections can thus be large enough to perhaps allow detection at LHC (note that the proposed cross sections for CEP of the SM Higgs boson are in some estimations of the order of 0.1 fb). The dependence on $\tan\beta$ shown in Fig. 5(b) is not as strong, but smaller values closer to the lower limit yield larger cross sections. The dependence on the charged Higgs mass shown in Fig. 5(c) is not strong within the limits, and it might be possible to consider larger values than we have done here, where we specialize to light $H^{\pm}$. The $CP$-odd Higgs mass, shown in Fig. 5(d), on the other hand, is preferred to be between 100 GeV and 250 GeV. For higher masses, the theoretical constraints on the Higgs potential become important and reduce the available parameter space. The drop in cross sections below 100 GeV is reflected in Fig. 5(a), where the structure at $\sigma \sim 10^{-2}$ fb at small $\sin(\beta - \alpha)$ corresponds to lower $m_{A^0}$.

To summarize the parameter scans, there are regions of parameter space of our selected prototype model where the cross sections are large enough to conceivably allow detection at the LHC.

## VI. DETECTION PROSPECTS, BACKGROUNDS

Experimentally, CEP will be searched for in high luminosity running at LHC with the help of forward proton detectors. We only consider the LHC at 14 TeV, since the luminosity at 7 TeV will not be large enough. One might expect that detection at high luminosity would be complicated by pileup, but it has been shown that, at least for $H \to b\bar{b}$, this problem can be overcome through careful cuts and vertex reconstruction [34]. Pileup can also be reduced by timing measurements of the forward protons [5].

The mass reconstruction of the central system is effective regardless of the decay channels of the central system. Since only forward, small angle scattering is considered, the outgoing protons will have small transverse momenta, so that also the centrally produced system has a small transverse momentum. The charged Higgs and the $W$

boson will therefore be more or less back-to-back. Since we are interested in higher masses of the central system than the canonical 120 GeV, the suggested forward detectors at 220 m in addition to the ones at 420 m would increase the acceptance [35].

The main decay channels of a light charged Higgs boson (light meaning lighter than the top quark) in the type I and II models are $H^+ \to \tau^+ \nu$ and $H^+ \to c\bar{s}$. There are therefore several possible scenarios. If both the $H^+$ and the $W$ decay leptonically, there will be a large amount of missing energy due to the neutrinos, together with a $\tau$ and a lepton. If they both decay hadronically, there will be four jets. If $m_{H^+}$ is close to $m_W$, special care may be needed to distinguish the associated production process from a SM Higgs that decays into $W^+W^-$ [36].

If one should consider the NMSSM, the decay channel $H^+ \to W^+ A_1$ can be prominent, since $A_1$ is light in many regions of parameter space. Here $A_1$ is the lightest of the CP-odd neutral Higgs bosons. (In a few points in our parameter space the decay $H^+ \to W^+ A^0$ is also significant, but these points have low cross sections.)

There is much less background to the associated production signal than to the SM $H \to b\bar{b}$ signal, where there is an irreducible $b\bar{b}$ background. Backgrounds that may need to be considered include the $gg \to W +$ jets, $gg \to WW$, $\gamma\gamma \to WW$ and $\gamma\gamma \to W\ell\nu$ processes considered in [36]. Thus, even if the associated production cross section is smaller than the SM Higgs cross section, the significance for $H^+W^-$ could be as large or even larger.

## VII. CONCLUSIONS AND OUTLOOK

In this paper we have proposed a novel central exclusive production mechanism for charged Higgs bosons in association with a $W$ boson. We have computed the cross section for this channel in prototype two-Higgs doublet models with light charged Higgs bosons. We have performed a limited parameter scan over the parameters of the model and have found that in some parts of parameter space, where the mixing of the $CP$-even Higgs bosons is small, the cross sections can be large enough to allow detection at LHC.

In the NMSSM, the charged Higgs boson is allowed to be rather light, and as our calculations using the type II 2HDM show, the associated CEP cross section can be almost as large as the SM Higgs production. It would therefore be very interesting to investigate this process in the NMSSM.

## ACKNOWLEDGMENTS

We thank Gunnar Ingelman, Oscar Stål and Antoni Szczurek for useful discussions. This work was supported by the Swedish Research Council under Contract No. 2007-4071 and by the Carl Trygger Foundation.

[1] J. F. Gunion, H. E. Haber, G. L. Kane, and S. Dawson, *The Higgs Hunter's Guide* (Perseus, Cambridge, 1990), 2nd ed..
[2] A. Djouadi, Phys. Rep. **459**, 1 (2008).
[3] A. Bialas and P. V. Landshoff, Phys. Lett. B **256**, 540 (1991).
[4] M. G. Albrow, T. D. Coughlin, and J. R. Forshaw, Prog. Part. Nucl. Phys. **65**, 149 (2010).
[5] M. G. Albrow and A. Rostovtsev, arXiv:hep-ph/0009336.
[6] M. G. Albrow *et al.* (FP420 R and D Collaboration), JINST**4**, T10001 (2009).
[7] J. R. Cudell and O. F. Hernandez, Nucl. Phys. **B471**, 471 (1996).
[8] V. A. Khoze, A. D. Martin, and M. G. Ryskin, Phys. Lett. B **401**, 330 (1997); V. A. Khoze, A. D. Martin, and M. G. Ryskin, Eur. Phys. J. C **14**, 525 (2000); V. A. Khoze, A. D. Martin, and M. G. Ryskin, Eur. Phys. J. C **19**, 477 (2001); **20**, 599(E) (2001); V. A. Khoze, A. D. Martin, and M. G. Ryskin, Eur. Phys. J. C **23**, 311 (2002); A. B. Kaidalov, V. A. Khoze, A. D. Martin, and M. G. Ryskin, Eur. Phys. J. C **33**, 261 (2004).
[9] R. Pasechnik, A. Szczurek, O. Teryaev, Phys. Rev. D **83**, 074017 (2011); **81**, 034024 (2010); Phys. Lett. B **680**, 62 (2009); Phys. Rev. D **78**, 014007 (2008); L. A. Harland-Lang, V. A. Khoze, and M. G. Ryskin *et al.*, Eur. Phys. J. C **69**, 179 (2010).
[10] J. R. Cudell, A. Dechambre, and O. F. Hernandez *et al.*, Eur. Phys. J. C **61**, 369 (2009).
[11] R. Maciula, R. Pasechnik, and A. Szczurek, Phys. Lett. B **685**, 165 (2010); Phys. Rev. D **82**, 114011 (2010); arXiv:1011.5842.
[12] T. Aaltonen *et al.* (CDF Collaboration), Phys. Rev. Lett. **99**, 242002 (2007); ()**102**, 242001 (2009); (), Phys. Rev. D **77**, 052004 (2008).
[13] A. Dechambre, O. Kepka, C. Royon, and R. Staszewski, Phys. Rev. D **83**, 054013 (2011).
[14] E. Asakawa, O. Brein, and S. Kanemura, Phys. Rev. D **72**, 055017 (2005).
[15] S. L. Glashow and S. Weinberg, Phys. Rev. D **15**, 1958 (1977).
[16] M. Ciuchini, G. Degrassi, P. Gambino, and G. F. Giudice, Nucl. Phys. **B527**, 21 (1998).
[17] F. Mahmoudi and O. Stål, Phys. Rev. D **81**, 035016 (2010).
[18] M. Aoki, S. Kanemura, K. Tsumura, and K. Yagyu, Phys. Rev. D **80**, 015017 (2009).
[19] A. G. Akeroyd, A. Arhrib, and Q. S. Yan, Eur. Phys. J. C **55**, 653 (2008).

[20] R. Dermisek and J. F. Gunion, Phys. Rev. D **79**, 055014 (2009).

[21] F. Mahmoudi, J. Rathsman, O. Stål, and L. Zeune, Eur. Phys. J. C **71**, 1608 (2011).

[22] A. A. Barrientos Bendezú and B. A. Kniehl, Phys. Rev. D **59**, 015009 (1998); A. A. Barrientos Bendezú and B. A. Kniehl, Phys. Rev. D **61**, 097701 (2000).

[23] A. A. Barrientos Bendezu and B. A. Kniehl, Phys. Rev. D **63**, 015009 (2000).

[24] O. Brein, W. Hollik, and S. Kanemura, Phys. Rev. D **63**, 095001 (2001).

[25] T. Hahn, Comput. Phys. Commun. **140**, 418 (2001); T. Hahn and M. Perez-Victoria, Comput. Phys. Commun. **118**, 153 (1999); T. Hahn, Comput. Phys. Commun. **178**, 217 (2008).

[26] M. G. Ryskin, A. D. Martin, and V. A. Khoze, Eur. Phys. J. C **60**, 265 (2009).

[27] M. A. Kimber, A. D. Martin, and M. G. Ryskin, Phys. Rev. D **63**, 114027 (2001).

[28] A. D. Martin and M. G. Ryskin, Phys. Rev. D **64**, 094017 (2001).

[29] T. D. Coughlin and J. R. Forshaw, J. High Energy Phys. 01 (2010) 121.

[30] D. Eriksson, J. Rathsman, and O. Stål, Comput. Phys. Commun. **181**, 189 (2010).

[31] P. Bechtle, O. Brein, S. Heinemeyer, G. Weiglein, and K. E. Williams, Comput. Phys. Commun. **181**, 138 (2010).

[32] M. E. Peskin and T. Takeuchi, Phys. Rev. Lett. **65**, 964 (1990); Phys. Rev. D **46**, 381 (1992).

[33] G. W. Bennett *et al.* (Muon G-2 Collaboration), Phys. Rev. D **73**, 072003 (2006); S. M. Barr and A. Zee, Phys. Rev. Lett. **55**, 2253 (1985); K. m. Cheung, C. H. Chou, and O. C. W. Kong, Phys. Rev. D **64**, 111301 (2001); K. Cheung and O. C. W. Kong, Phys. Rev. D **68**, 053003 (2003).

[34] B. E. Cox, F. K. Loebinger, and A. D. Pilkington, J. High Energy Phys. 10 (2007) 090.

[35] S. Heinemeyer, V. A. Khoze, M. G. Ryskin, W. J. Stirling, M. Tasevsky, and G. Weiglein, Eur. Phys. J. C **53**, 231 (2007).

[36] B. E. Cox, A. De Roeck, and V. A. Khoze *et al.*, Eur. Phys. J. C **45**, 401 (2005).